Power Electronic Systems
Laboratory

IEEE Transactions on Power Electronics, Vol. 33, No. 1, pp. 4-7, January 2018

Generic Derivation of Dynamic Model for Half-Cycle DCM Series Resonant Converters

J. E. Huber,
J. Miniböck,
J. W. Kolar

Eidgenössische Technische Hochschule Zürich
Swiss Federal Institute of Technology Zurich

Generic Derivation of Dynamic Model for Half-Cycle DCM Series Resonant Converters

Jonas E. Huber, *Member, IEEE,* Johann Miniböck, and Johann W. Kolar, *Fellow, IEEE*

***Abstract*—The series resonant converter (SRC) operated in the half-cycle discontinuous-conduction-mode (HC-DCM) provides galvanic separation and a tight coupling of its input and output voltages in open-loop operation, i. e., with minimum control complexity, which renders it suitable for a wide range of applications that require galvanic isolation. This letter first explains the "DC transformer" behavior of the converter and then provides a generic derivation of a passive equivalent circuit that accurately models the converter's terminal behavior. The proposed generic derivation yields the known analytic results for idealized cases, but additionally allows for a parametrization of the equivalent circuit based on simulated or measured waveforms, thereby facilitating high accuracy also in non-ideal cases. Furthermore, it is shown that a non-infinite magnetzining inductance results in an additional load-independent difference between the input and the output voltage, and a corresponding extension of the equivalent circuit model is proposed. The considerations are verified by simulations and measurements of a 10 kW / 350 V / 350 V HC-DCM SRC system.**

***Index Terms*—Series resonant converters, half-cycle discontinuous conduction mode, dynamic equivalent circuit.**

I. Introduction

THERE are converter systems that employ a dedicated stage to provide galvanic separation and voltage scaling, whereas the power flow is controlled by another stage in the power conversion path (e. g., [1], [2]). In such applications, minimum complexity of the isolation stage is desirable. The series resonant converter (SRC) operated in the half-cycle discontinuous-conduction-mode (HC-DCM) [3]–[5] is of high interest for such applications, because it achieves a tight coupling of its input and output voltages in open-loop operation, while providing zero-current switching (ZCS) and potentially also load-independent zero-voltage switching (ZVS) utilizing the magnetizing current [6].

A. Operating Principle of the HC-DCM SRC

Fig. 1a shows a generic representation of a HC-DCM SRC, and Fig. 1b shows key waveforms for a single switching period. For power transfer from the input to the output, only the input-side bridge is actively switched to generate a rectangular voltage, v_{B1}, with a switching frequency $f_{\mathrm{s}} \leq f_0 = 1/(2\pi\sqrt{L_\sigma C_{\mathrm{r}}})$ and (almost) full duty ratio, which is applied to the resonant tank formed by the transformer's stray inductance, L_σ, and a series resonant capacitor, C_{r}.

J. E. Huber and J. W. Kolar are with the Power Electronic Systems Laboratory of ETH Zurich, 8092 Zürich, Switzerland. (e-mail: huber@lem.ee.ethz.ch, kolar@lem.ee.ethz.ch).

J. Miniböck is with m-pec power electronics consulting, Walkenstein, Austria. (e-mail: miniboeck@mpec.at).

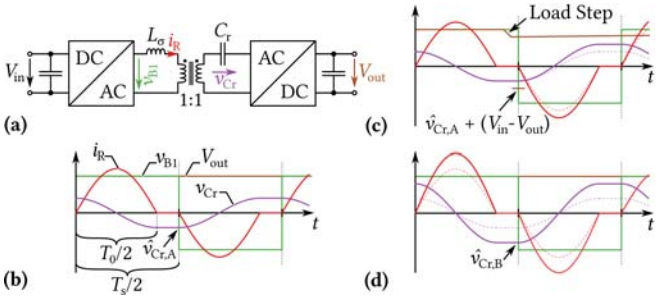

Fig. 1. (a) Basic HC-DCM SRC topology, (b) idealized waveforms for a steady state A, (c) disturbance of this steady state by a load current step that causes a sag of the output voltage, and (d) new steady state B with a power flow adapted to the increased load.

Considering a lossless case, i. e., ideal components, the steady-state output voltage equals the input voltage (scaled by the transformer turns ratio, which is assumed to be $n = 1$ here). At the beginning of a new switching half-cycle, therefore only the voltage across the resonant capacitor, $\hat{v}_{\mathrm{Cr}}$, excites the resonant tank and gives rise to a sinusoidal current pulse according to

$$i_{\mathrm{R}}(t) = \frac{\hat{v}_{\mathrm{Cr}}}{Z_0} \sin(\omega_0 t) \text{ for } t \leq T_0/2, \tag{1}$$

where $Z_0 = \sqrt{L_\sigma / C_{\mathrm{r}}}$ and $\omega_0 = 2\pi f_0$. Since the second bridge is operated as a diode rectifier, the current cannot reverse its direction once it reaches zero at $t = T_0/2$, where $T_0 = 1/f_0$. The resonant current pulse changes the voltage of C_{r} to $-\hat{v}_{\mathrm{Cr}}$ at $t = T_0/2$; it stays constant until the next switching cycle is initiated at $t = T_{\mathrm{s}}/2$. The negative half-cycle follows from symmetry considerations.

B. Idealized "DC Transformer" Behavior

The HC-DCM SRC acts as a "DC Transformer" by tightly coupling its input and output voltages as mentioned above. Still considering ideal components, i. e., no losses, this behavior can be explained starting from a certain steady state A with a given power flow through the converter and $V_{\mathrm{out}} = V_{\mathrm{in}}/n$ as shown in Fig. 1b. Then, the excitation voltage of each resonant pulse is given by the peak resonant capacitor voltage, i. e., $\hat{v}_{\mathrm{Cr,A}}$, and hence $\hat{i}_{\mathrm{R}} = \hat{v}_{\mathrm{Cr,A}}/Z_0$.

If the load current changes abruptly, the output voltage sags in case of a non-infinite output capacitance, as it is shown in Fig. 1c. However, then the temporary difference between the output and the input voltage will also contribute to the excitation voltage of the next resonant cycle, i. e., it becomes $\hat{v}_{\mathrm{Cr,A}} + (V_{\mathrm{in}} - V_{\mathrm{out}}) > \hat{v}_{\mathrm{Cr,A}}$. Accordingly, the amplitude of this next resonant current pulse will be higher,

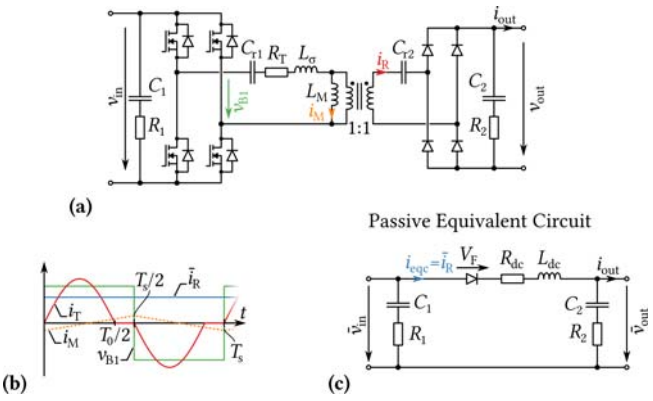

Fig. 2. (a) Considered series resonant converter topology; (b) key waveforms; (c) dynamic passive equivalent circuit.

which corresponds to an increase of the power transfer through the converter—the power flow is automatically adjusted to meet the higher load at the output until finally a new steady state B with a corresponding higher power transfer is attained (Fig. 1d). Note that the series resistances as well as the forward voltage drops of the power semicondcutors in the current path of a real converter cause an additional (load-dependent) voltage difference between the input and the output voltage.

C. Dynamic Equivalent Circuit

The dynamics of this "DC transformer" behavior of the HC-DCM SRC with respect to its terminal voltages and currents can be accurately modeled by a passive equivalent circuit, which is based on the local average value (over half a switching period), $\bar{i}_\mathrm{R}$, of the real converter's resonant current, i_R (cf. Fig. 2ab). Such an equivalent circuit has been proposed already in 1990 [7], [8] for sinusoidal currents and was then refined later considering piece-wise sinusoidal currents [9], [10] (both in German). However, the equivalent circuit model can also be derived in a very generic way using power- and energy considerations [1]. This facilitates a parametrization of the model not only by means of calculations, but also directly from simulated or measured converter waveforms, which allows to easily employ the model for systems with non-standard current shapes (e. g., for converters with small DC capacitors, where the pulse shape deviates from a piecewise sinusoid [11]). Since the HC-DCM SRC is often employed as an isolation stage within a system consisting of several converter stages, such an emipircal parametrization using simulation or measurement results can be valuable in order to assess the effect of the SRC's dynamics on those of the complete system, e. g., by means of its transfer function that can be easily derived from the passive equivalent circuit. In the following, the generic derivation of the equivalent circuit is explained and verified by simulations and experiments. Furthermore, the magnetizing inductance's impact on the model accuracy is analyzed and a corresponding extension of the model is proposed.

II. Generic Derivation of the Equivalent Circuit

Generally, a given power flow through the SRC is associated with certain (conduction) losses and a certain amount of stored energy in the resonant tank. In order for the equivalent circuit model to accurately mimic the switched system's terminal behavior, its losses and its stored energy must be equal to those of the switched system for the same power flow. These two simple power- and energy-related conditions are sufficient to derive the parameters of the equivalent circuit in Fig. 2c.

A. Equal Load-Dependent Losses

The load-dependent losses occur in the power semiconductors, which are modeled as a on-state resistance, r_on, and in case of diodes or IGBTs by an additional voltage source, v_0, as well as in other series resistances, such as the transformer windings.

Losses resulting from v_0 depend on the average current through the semiconductors. Since the local average current, $\bar{i}_\mathrm{R}$, is flowing in the equivalent circuit, a diode with an equivalent voltage drop can model these losses. The equivalent voltage drop, V_F, corresponds to the sum of all voltage drops in the current path, i. e., $V_F = 2v_{0,\mathrm{diode}}$ in the considered circuit.

In contrast, the load-dependent losses caused by the total series resistance in the current path, R_total, depend on the rms current of the switched converter, $\tilde{i}_\mathrm{R}$. Because the resistance in the equivalent circuit, R_dc, is only exposed to the local average current, it must be adapted in order to yield equal losses:

$$\bar{i}_R^2 R_\mathrm{dc} \overset{!}{=} \tilde{i}_\mathrm{R}^2 R_\mathrm{total} \;\Rightarrow\; R_\mathrm{dc} = \beta^2 R_\mathrm{total} \text{ with } \beta^2 := \frac{\tilde{i}_\mathrm{R}^2}{\bar{i}_\mathrm{R}^2}. \quad (2)$$

The series resistances of the DC bus capacitors are included in the equivalent model, where they retain their effect on the terminal currents; however, in a switched system they would also be exposed to the resonant current, resulting in corresponding rms losses. To account for this, R_dc can be adapted [9]:

$$R_\mathrm{dc} = \beta^2 R_\mathrm{total} + (\beta^2 - 1)(R_1 + R_2). \quad (3)$$

Note that switching losses and core losses do not depend strongly on the transferred power in DCM mode. Therefore, they do not contribute to the converter dynamics. Nevertheless, it would be possible to model these losses with shunt resistors in the equivalent circuit, if desired.

B. Equal Load-Dependent Stored Energy

The energy stored in the resonant tank, E_stor, depends on the transferred power according to

$$E_\mathrm{stor} = \frac{1}{2} L_\sigma \hat{i}_\mathrm{R}^2 \text{ with } \hat{i}_\mathrm{R} = f(P). \quad (4)$$

Because the inductor in the equivalent circuit, L_dc, is only exposed to the local average current, it must be adapted in order to yield equal stored energy:

$$\bar{i}_\mathrm{R}^2 L_\mathrm{dc} \overset{!}{=} \hat{i}_\mathrm{R}^2 L_\sigma \;\Rightarrow\; L_\mathrm{dc} = \alpha^2 L_\sigma \text{ with } \alpha^2 := \frac{\hat{i}_\mathrm{R}^2}{\bar{i}_\mathrm{R}^2}. \quad (5)$$

As an aside, note that if a converter bridge is realized as a half-bridge, the DC capacitor in the equivalent circuit has to be adapted such that the stored energy remains the same [1].

TABLE I
SPECIFICATIONS OF EXAMPLE SYSTEM AND PROTOTYPE.

Rated power	10 kW	$C_{r1} = C_{r2}$	1 µF
Rated input voltage	350 V	L_σ	19.2 µH
Rated output voltage	350 V	R_T	204 mΩ
Switching freq., f_s	ca. 50 kHz	$C_1 = C_2$	15 µF
n	1	L_M	300 µH

TABLE II
WAVEFORM PARAMETER EXTRACTION FORM SIMULATION.

	Ideal (calc.)	Large DC Cap.	Small DC Cap.
$\hat{i}_R$	–	45.14 A	47.12 A
$\tilde{i}_R$	–	31.37 A	31.94 A
$\bar{i}_R$	–	27.78 A	27.69 A
α	1.61	1.62	1.70
β	1.13	1.13	1.15
L_{dc}	50.0 µH	50.7 µH	55.6 µH
R_{dc}	262 mΩ	264 mΩ	276 mΩ

C. Summary and Discussion

For the case of (piecewise) sinusoidal current, simple analytic expressions for α and β can be found [9]:

$$\alpha = \frac{\pi}{2}\frac{f_0}{f_s} \quad \text{and} \quad \beta = \frac{\pi}{2\sqrt{2}} \cdot \sqrt{\frac{f_0}{f_s}}. \tag{6}$$

However, the two ratios,

$$\alpha := \frac{\hat{i}_R}{\bar{i}_R} \quad \text{and} \quad \beta := \frac{\tilde{i}_R}{\bar{i}_R}, \tag{7}$$

can be defined for arbitrary current shapes, i. e., in particular they can be calculated from simulated or measured current waveforms. This illustrates the highly generic nature of the proposed power- and energy-based derivation of the equivalent circuit.

III. VERIFICATION BY SIMULATION

Considering the specifications given in Table I but for now neglecting the magnetizing inductance, L_M, it is possible to calculate idealized α and β using (6). Table II shows the results, which are very close to those obtained from simulated waveforms of the switched system. There, the rms, peak and average values of the resonant current are extracted from a steady-state simulation and given in Table II; α and β can then be calculated using (7). Fig. 3a illustrates that the equivalent circuit models the converter dynamics accurately.

If smaller DC capacitors are considered (i. e., about $C_{dc} < 10C_r$, specifically 1.5 µF instead of 15 µF), the calculation of α and β would become very complicated [1]. It is much more straightforward to extract the parameters from simulated waveforms, as shown in Table II. Note that the resulting equivalent circuit element values deviate significantly from the ones calculated for large DC capacitors, whereas the correspondingly parametrized equivalent circuit still captures the terminal behavior accurately (cf. Fig. 3b).

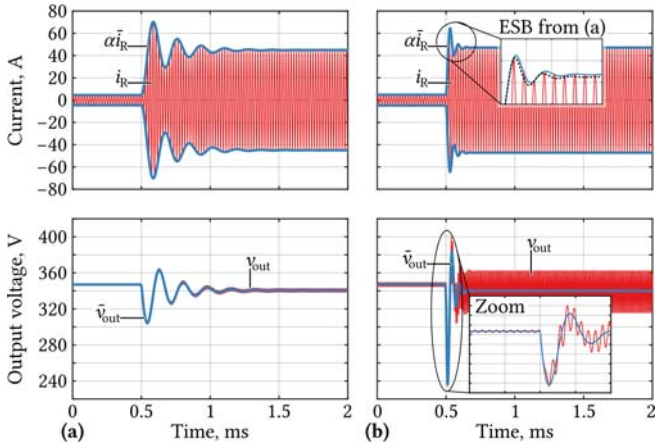

Fig. 3. Resonant current (top) and output voltage (bottom) from switched simulation (with $L_M \to \infty$) and from equivalent circuit (a) for $C_1 = C_2 = 15$ µF (i. e., comparatively large DC link capacitors) and (b) for $C_1 = C_2 = 1.5$ µF (i. e., comparatively small DC link capacitors).

IV. INFLUENCE OF MAGNETIZING INDUCTANCE

A non-infinite magnetizing inductance, L_M, corresponds to a non-ideal coupling of the two transformer windings, which causes an additional voltage difference between the converter's input and output voltages. Considering the circuit from Fig. 2a, the stray inductance L_σ would be fully compensated by C_{r1} if $f_s = f_0$, and if only a single series capacitor on the active side would be employed ($C_{r2} \to \infty$). Else, i. e., under typical operating conditions where $f_s < f_0$, the resulting residual series impedance $\underline{Z}_s = \underline{Z}_{L\sigma} + \underline{Z}_{Cr1}$ (neglecting the typically small series resistances) forms a voltage divider with the non-infinite magnetizing impedance, $\underline{Z}_M$, giving rise to an additional voltage difference, Δv, between the input and the output voltage:

$$\frac{\Delta v}{V_{in}} = \frac{\underline{Z}_s}{\underline{Z}_s + \underline{Z}_M} = \frac{j\omega_s L_\sigma + 1/(j\omega_s C_{r1})}{j\omega_s L_\sigma + 1/(j\omega_s C_{r1}) + j\omega_s L_M}. \tag{8}$$

Note that $\Delta v / V_{in} = 0$ for $L_M \to \infty$.

Especially for lower ratios L_M/L_σ also the shape of the current pulses is affected, i. e., it becomes necessary to extract α and β from a simulation or a measurement. This has been done for a set of configurations, and the resulting output voltage deviations between the switched simulation and the equivalent circuit (without modeling Δv yet) are shown in Fig. 4, confirming that (8) is a good approximation of the additional voltage difference caused by the magnetizing inductance. Furthermore, this deviation becomes small ($< 5\,\%$) for ratios $L_M/L_\sigma > 10$ if f_s is chosen close to f_0 as is typically the case in order to minimize losses. Note that if a single resonant capacitor is employed, $\Delta v = 0$ V for $f_s = f_0$, independent of L_M/L_σ. This is not the case if the resonant capacitor is split, because the compensation of L_σ is not perfect even for $f_s = f_0$.

If required, the additional voltage difference can be incorporated in the equivalent circuit by means of an idealized diode (or, in bidirectional systems, a Zener diode) with a corresponding forward voltage drop (and reverse breakdown voltage). Alternatively, a voltage source may be used or the

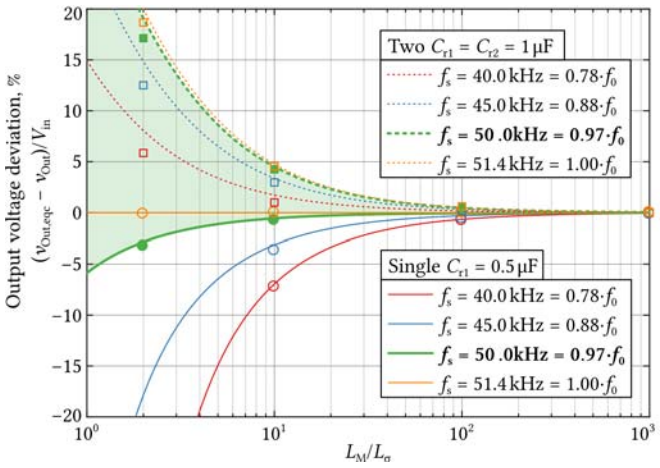

Fig. 4. Influence of the magnetizing inductance on the output voltage. The curves are calculated using (8), whereas circles and squares are obtained from comparing a full switched simulation including L_M with the results of an accordingly parametrized equivalent circuit that does not yet consider L_M (circles: single resonant capacitor C_{r1}; squares: two resonant capacitors $C_{r1} = C_{r2}$).

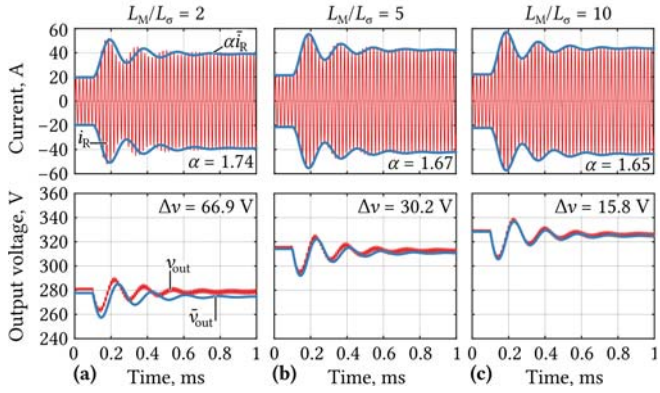

Fig. 5. Impact of the ratio L_M/L_σ on the dynamic behavior: α, β, and hence L_{dc} and R_{dc} are extracted from (steady-state) simulations, Δv is calculated using (8) and implemented in the dynamic equivalent circuit accordingly. The transient behavior is modeled accurately for common ratios of $L_M/L_\sigma \geq 5$, cf. (b) and (c).

input voltage may be adapted accordingly. In the input to output voltage transfer function, the voltage difference appears as a constant factor smaller than unity.

Fig. 5 shows simulated step responses for three different L_M values. As discussed above, the equivalent circuit is parametrized from the simulated waveforms and Δv is caluclated using (8) for each case, resulting in good steady-state accuracies. For very low ratios of L_M/L_σ, the dynamics obtained from the equivalent circuit are slightly too slow (cf. Fig. 5a), which is an effect not captured by the equivalent circuit. However, the practical relevance of this is limited, since for common ratios of $L_M/L_\sigma \geq 5$, the impact is completely negligible as illustrated by the waveforms in Fig. 5bc.

V. Experimental Verification

In order to show the proposed dynamic model's ability to accurately describe the terminal behavior of a real SRC, the

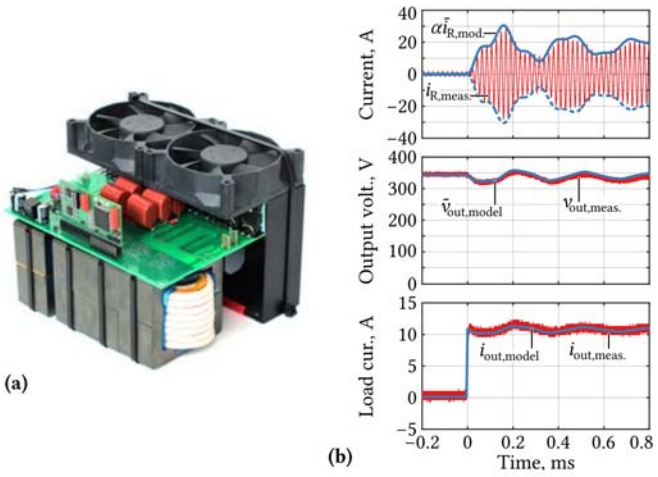

Fig. 6. (a) HC-DCM SRC prototype rated at 10 kW / 350 V / 350 V; (b) comparison of measured step response and predictions from the passive equivalent circuit. The prototype's dimensions are 160 mm × 140 mm × 120 mm; it employs Infineon's 650 V CoolMOS CFD2 MOSFETs (IPW65R041CFD) on the primary side and 600 V HFA50PA60C fast recovery diodes on the secondary side. The transformer is built with three E70 ferrite cores using 8 turns of 350 × 0.2 mm litz wire, and a fourth core is used to realize the required total series inductance (L_σ).

load step response of a prototype system shown in Fig. 6a is compared to the model in the following by first parametrizing the equivalent cirucit based on steady-state measurements and then simulating the same step response as has been measured with the prototype. The prototype's specifications are given in Table I; it features a peak efficiency above 98 % and a power density typical for industrial systems. During the experiments, an input DC voltage of 355 V is used and the switching frequency is set to 47.6 kHz (to optimize the ratio f_0/f_s regarding losses). Furthermore, a decoupling inductor with an inductance of 58 µH is placed between the power supply and the input terminals of the SRC, which can be added in the same way to the equivalent circuit simulation, since it is an external component.

To parametrize the equivalent circuit elements, the ratios α and β are calculated from the characteristic values of the measured steady-state current waveform. With (7) and the measured values for $\hat{i}_R = 42.12$ A, $\tilde{i}_R = 29.35$ A and $\bar{i}_R = 26.06$ A, directly $\alpha = 1.62$ and $\beta = 1.13$ follow, which are very close to the values obtained through calculation or simulation given in Table I. From that, the equivalent circuit elements can be calculated as $L_{dc} = 50.2\,\mu H$ and $R_{dc} = 262.4\,m\Omega$. Furthermore, the ratio between magnetizing inductance and stray inductance is $L_M/L_\sigma = 15.6$, which, according to (8), yields an additional voltage drop of $\Delta v = 9.2$ V (2.6 %). This is considered in the simulated equivalent circuit by means of an additional series diode.

Fig. 6b shows a measured load step response (from zero to about 3.5 kW) as well as the corresponding results from the equivalent circuit model simulation. The comparison illustrates that the dynamic model can be easily parametrized from measurements of a real system and then be employed to accurately predict the real system's terminal behavior.

VI. Conclusion

This letter proposes a generic derivation of the passive equivalent circuit model of the half-cycle discontinuous-conduction-mode (HC-DCM) series resonant converter (SRC). The generic approach yields the known analytic results for ideal cases, but facilitates also a parametrization based on simulated or measured converter waveforms, whereby non-idealities are easily considered. Furthermore, the influence of a non-infinite magnetizing inductance is analyzed and a corresponding extension of the equivalent circuit is proposed. Finally, experimental results of a 10 kW / 350 V / 350 V HC-DCM SRC confirm the accuracy of the dynamic equivalent circuit model and illustrate the effectiveness of the measurement-based parametrization that is enabled by the proposed generic derivation of the equivalent circuit model.

References

[1] J. E. Huber and J. W. Kolar, "Analysis and design of fixed voltage transfer ratio DC/DC converter cells for phase-modular solid-state transformers," in *Proc. IEEE Energy Conversion Congr. and Expo. (ECCE)*, Montréal, QC, Canada, Sep. 2015, pp. 5021–5029.

[2] C. Swartz, "High performance ZVS buck regulator removes barriers to increased power throughput in wide input range point-of-load applications," VICOR White Paper, 2012. [Online]. Available: http://goo.gl/YZ1A8e

[3] W. McMurray, "Multipurpose power converter circuits," U.S. Patent 3,487,289, Dec., 1969.

[4] ——, "The thyristor electronic transformer: a power converter using a high-frequency link," *IEEE Trans. Ind. Gen. A.*, vol. IGA-7, no. 4, pp. 451–457, Jul. 1971.

[5] F. C. Schwarz, "A method of resonant current pulse modulation for power converters," *IEEE T. Ind. El. Con. In.*, vol. IECI-17, no. 3, pp. 209–221, May 1970.

[6] J. Huber, G. Ortiz, F. Krismer, N. Widmer, and J. W. Kolar, "η-ρ Pareto optimization of bidirectional half-cycle discontinuous-conduction-mode series-resonant DC/DC converter with fixed voltage transfer ratio," in *Proc. 28th Annu. IEEE Applied Power Electron. Conf. and Expo. (APEC)*, Long Beach, CA, USA, Mar. 2013, pp. 1413–1420.

[7] A. Esser and H. C. Skudelny, "A new approach to power supplies for robots," *IEEE Trans. Ind. Appl.*, vol. 27, no. 5, pp. 872–875, Sep. 1991.

[8] A. Esser, "Berührungslose, kombinierte Energie- und Informationsübertragung für bewegliche Systeme (in German)," PhD Dissertation, RWTH Aachen, Aachen, Germany, 1992.

[9] M. Steiner, "Seriegeschaltete Gleichspannungszwischenkreisumrichter in Traktionsanwendungen am Wechselspannungsfahrdraht (in German)," PhD Dissertation, ETH Zurich, Zurich, Switzerland, 2000.

[10] D. Zuber, "Mittelfrequente resonante DC/DC-Wandler für Traktionsanwendungen (in German)," PhD Dissertation, ETH Zurich, Zurich, Switzerland, 2001.

[11] D. Rothmund, J. E. Huber, and J. W. Kolar, "Operating behavior and design of the half-cycle discontinuous-conduction-mode series-resonant-converter with small DC link capacitors," in *Proc. 14th IEEE Workshop on Control and Modeling for Power Electron. (COMPEL)*, Salt Lake City, UT, USA, Jun. 2013.